Nanoscale Res Lett (2008) 3:230–235
DOI 10.1007/s11671-008-9141-5

NANO EXPRESS

The Influences of H_2 Plasma Pretreatment on the Growth of Vertically Aligned Carbon Nanotubes by Microwave Plasma Chemical Vapor Deposition

Sheng-Rui Jian · Yuan-Tsung Chen · Chih-Feng Wang · Hua-Chiang Wen · Wei-Ming Chiu · Chu-Shou Yang

Received: 2 April 2008 / Accepted: 12 June 2008 / Published online: 24 June 2008

Abstract The effects of H_2 flow rate during plasma pretreatment on synthesizing the multiwalled carbon nanotubes (MWCNTs) by using the microwave plasma chemical vapor deposition are investigated in this study. A H_2 and CH_4 gas mixture with a 9:1 ratio was used as a precursor for the synthesis of MWCNT on Ni-coated TaN/Si(100) substrates. The structure and composition of Ni catalyst nanoparticles were investigated using scanning electron microscopy (SEM) and transmission electron microscopy (TEM). The present findings showed that denser Ni catalyst nanoparticles and more vertically aligned MWCNTs could be effectively achieved at higher flow rates. From Raman results, we found that the intensity ratio of G and D bands (I_D/I_G) decreases with an increasing flow rate. In addition, TEM results suggest that H_2 plasma pretreatment can effectively reduce the amorphous carbon and carbonaceous particles. As a result, the pretreatment plays a crucial role in modifying the obtained MWCNTs structures.

S.-R. Jian (✉) · Y.-T. Chen · C.-F. Wang
Department of Materials Science and Engineering, I-Shou University, No.1, Sec.1, Syuecheng Rd., Dashu Township, Kaohsiung 840, Taiwan, ROC
e-mail: srjian@gmail.com

H.-C. Wen
Department of Electrophysics, National Chiao Tung University, Hsinchu 300, Taiwan, ROC

W.-M. Chiu
Department of Chemical and Materials Engineering, National Chin-Yi University of Technology, Taichung 411, Taiwan, ROC

C.-S. Yang
Graduate Program in Electro-Optical Engineering, Tatung Universiy, Taipei 10452, Taiwan, ROC

Keywords Multiwalled carbon nanotubes · H_2 pretreatment · Raman spectroscopy · Scanning electron microscopy · Transmission electron microscopy

Introduction

Carbon nanotubes (CNTs) [1] undoubtedly occupy a unique position among advanced materials because of its novel electrical, mechanical, and chemical characteristics [2–4]. With these useful properties, CNTs are good candidates for various applications, such as field-effect transistors [5], sensors [6], field-emission displays [7, 8], and nanoscale interconnects [9].

CNTs can be synthesized by a variety of techniques, such as arc discharge, laser ablation, and plasma-enhanced and thermal chemical vapor depositions (CVDs) [10–13]. Although the former two techniques are suitable for large-scale production of CNTs, they cannot be used for self-assembly on material surfaces. CNTs synthesized by CVD are known to be longer than those obtained by other processes. It is possible to grow dense arrays of aligned CNTs by CVD [14], as well. Therefore, CVD is one of the prominent methods for synthesizing high-purity, high-yield CNTs for practical applications. Meanwhile, control of the CNT structure has a technical advantage in that the structural diversity leads to different electronic and mechanical characteristics. Several attempts have been made to control the structure of CNTs by various methods, including the pretreatment of the metal films on which CNTs are grown [15] and the direct control of structure by varying synthesis parameters [16]. In particular, plasma etching can be used to transform a catalytic layer into catalytic nanoparticles, which might be applied to the density control of CNTs. In addition, however, to avoid the formation of metal silicide

at a high temperature, a buffer layer was adopted in the annealing process [17].

In this study, the effects of H_2 flow rate during plasma pretreatment on the synthesis of MWCNTs on a Ni/TaN/Si substrate by using a microwave plasma chemical vapor deposition (MPCVD) system are investigated. The structure and composition of Ni catalyst nanoparticles are investigated by using scanning electron microscopy (SEM) and transmission electron microscopy (TEM). Raman spectroscopy equipped with a charge-coupled device detector is used to study the effect of flow rate on the intensity ratio of G and D bands (I_D/I_G), which, in turn, measures the amounts of the amorphous carbon and carbonaceous particles in the MWCNTs.

Experimental Details

The substrates used in the experiments were 6-inch p-Si(100) wafers which were cleaned using standard RCA cleaning procedures to remove chemical impurities and particles. For the growth of MWCNTs, three steps were followed: (1) a 7-nm layer of nickel (Ni) and a 20-nm layer of tantalum nitride (TaN) were deposited on the substrate in a PVD system (800 W at a sputtering pressure of 6.4×10^{-3} torr). (2) the Ni-coated substrate was submitted to a procedure called hereafter as pretreatment, which consisted of its annealing at 550 °C for 10 min in a H_2 plasma. The pretreatment was performed at different H_2 flow ratios (100, 200, and 300 sccm) in a 915-MHz microwave plasma chemical vapor deposition (MPCVD) system. This procedure converted the Ni layer in Ni nanoparticles distributed on the substrate surface. (3) Methane gas was then admitted in the plasma chamber (90 sccm H_2 and 10 sccm CH_4) for the CNTs growth with the substrate kept at 550 °C for 10 min (The total pressure in the chamber was kept at 20 torr, while the gas flow rates were increased at step 2 and 3). Ni catalyst nanoparticles were examined by scanning electron microscopy (SEM, Hitachi S-4000) and high-resolution transmission electron microscopy (HRTEM, JEOL, JEM-2100F). Synthesis of aligned MWCNTs was investigated by means of SEM and TEM. In addition, Raman spectroscopy was performed in a Renishaw 1000 Spectrometer equipped with a charge-coupled device detector and operated at a wavelength of 514.5 nm and at a power of 100 mW.

Results and Discussion

In this study, we confirm the strong dependence of the catalyst morphology on the process parameters. In previous results, there were evidences that the morphology of the catalyst was dependent on the H_2 plasma treatment time [18], H_2 concentration [19], and H_2 gas flow rate [20]. In this article, we kept the substrate temperature (550 °C) and treatment time (10 min) the same as in the prior report [20] and choose the H_2 flow rate as the single parameter. The synthesis of MWCNTs by CVD often involves three main steps: (1) decomposition of hydrocarbon gas at the surface of the catalyst nanoparticles; (2) diffusion of resultant carbon atom in the nanoparticles to form the nucleation seed; and (3) precipitation of carbon atoms at the nanoparticle interface to form MWCNTs. It is well known and often proposed that the size and chemical composition of metal nanoparticles determine the diameter and structural nature of the MWCNTs [21].

Ni catalyst metal layers transformed into nanoparticles after various H_2 flows rate during plasma pretreatment are illustrated in Fig. 1. From this figure, it is clearly observed that higher H_2 flow rate during plasma pretreatment lead to denser Ni catalyst nanoparticles. With etching by H_2 plasma, the Ni catalyst metal layers break into small islands. SEM observations confirm that the H_2 plasma pretreatment plays an important role in promoting the uniform formation of Ni nanoparticles. The particle sizes of Ni catalyst metal layers treated by H_2 plasma etching are about 20–30 nm, which are displayed in the cross-sectional TEM images in Fig. 2. It is interesting to note that the geometries of the Ni catalyst particles were obviously affected by the H_2 flow rate during plasma pretreatment. As shown in Fig. 2, at the flow rates of 100 and 200 sccm, the Ni catalyst particles have broad-based shapes, whereas at a flow rate of 300 sccm, the Ni catalyst particle has a semicircle-like shape. Such a morphology difference is not surprising because at a higher flow rate, the atoms in the catalyst particle can move around more easily via H_2 plasma etching than at a lower flow rate. In the plasma environment, the H_2 plasma plays a role in reducing Ni nanoparticles as suggested in Ref. [22]. These observations also indicate that the geometry of a large catalyst particle can be reshaped more easily at a higher flow rate for the MWCNTs nucleation and growth.

Figure 3 shows the cross-sectional SEM images of the MWCNTs grown at a 90 sccm H_2/10 sccm methane composition based on the three different pretreatments flow rates of 100, 200, and 300 sccm, respectively. Amorphous carbon and carbonaceous particles were decreased and denser vertically aligned MWCNTs were obtained for a higher flow rate pretreatment, as shown in Fig. 3. In addition, the MWCNTs shown in Fig. 3c were 30–40 nm in diameter and several micrometers in length. From this observation, the ability of Ni catalyst particles to change their shape can also explain why in the present experiment the highest density of MWCNTs was synthesized at the flow rate of 300 sccm. We confirmed that the Ni layer not

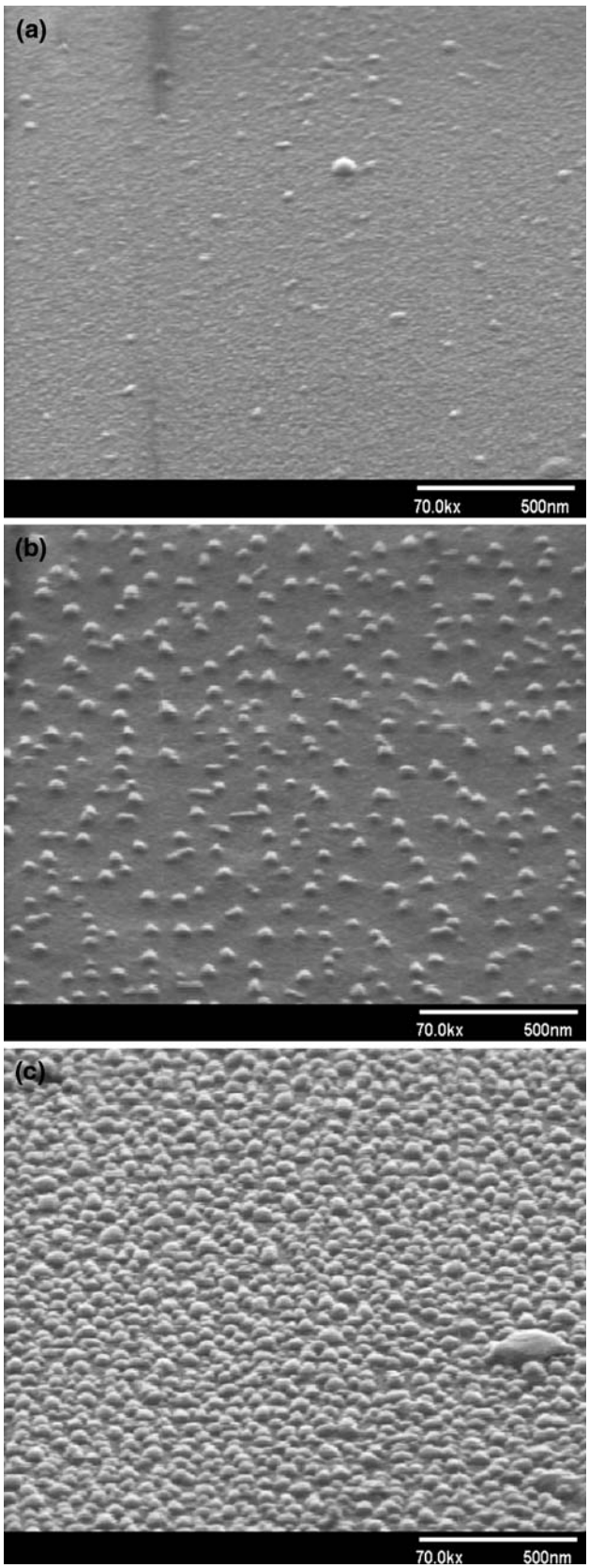

Fig. 1 SEM images of Ni catalyst nanoparticles at various H_2 flow rate during plasma pretreatment of (**a**) 100, (**b**) 200, and (**c**) 300 sccm

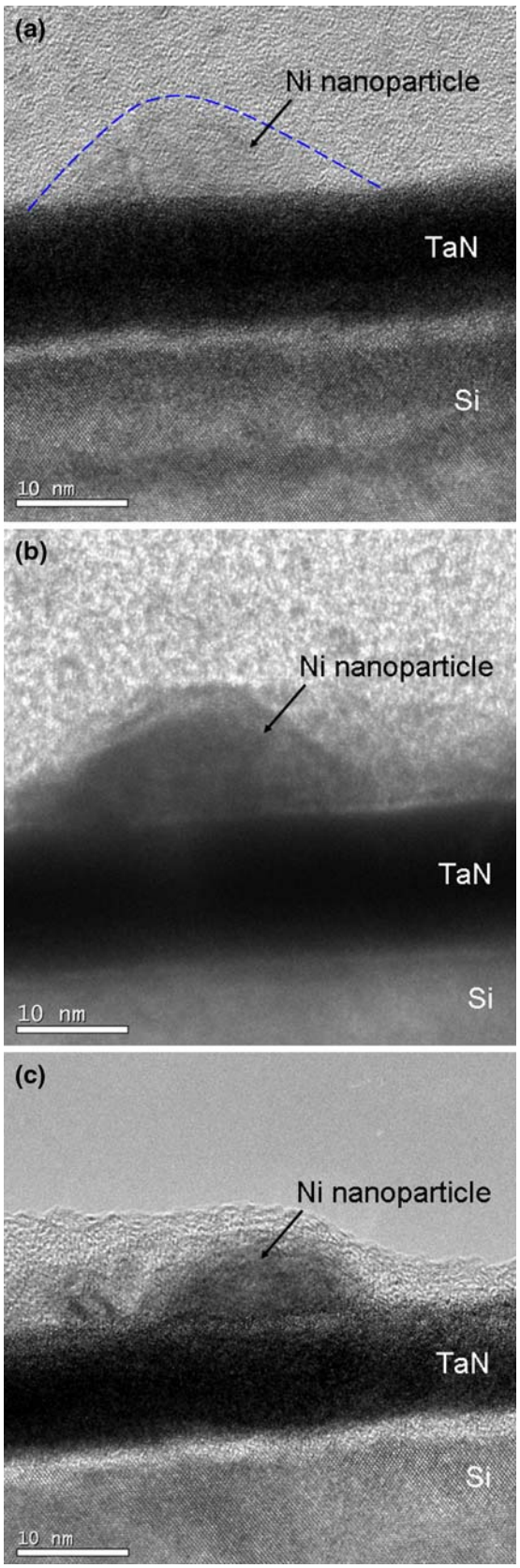

Fig. 2 TEM images of Ni catalyst nanoparticles with various H_2 flow rate during plasma pretreatment of (**a**) 100, (**b**), 200 and (**c**) 300 sccm

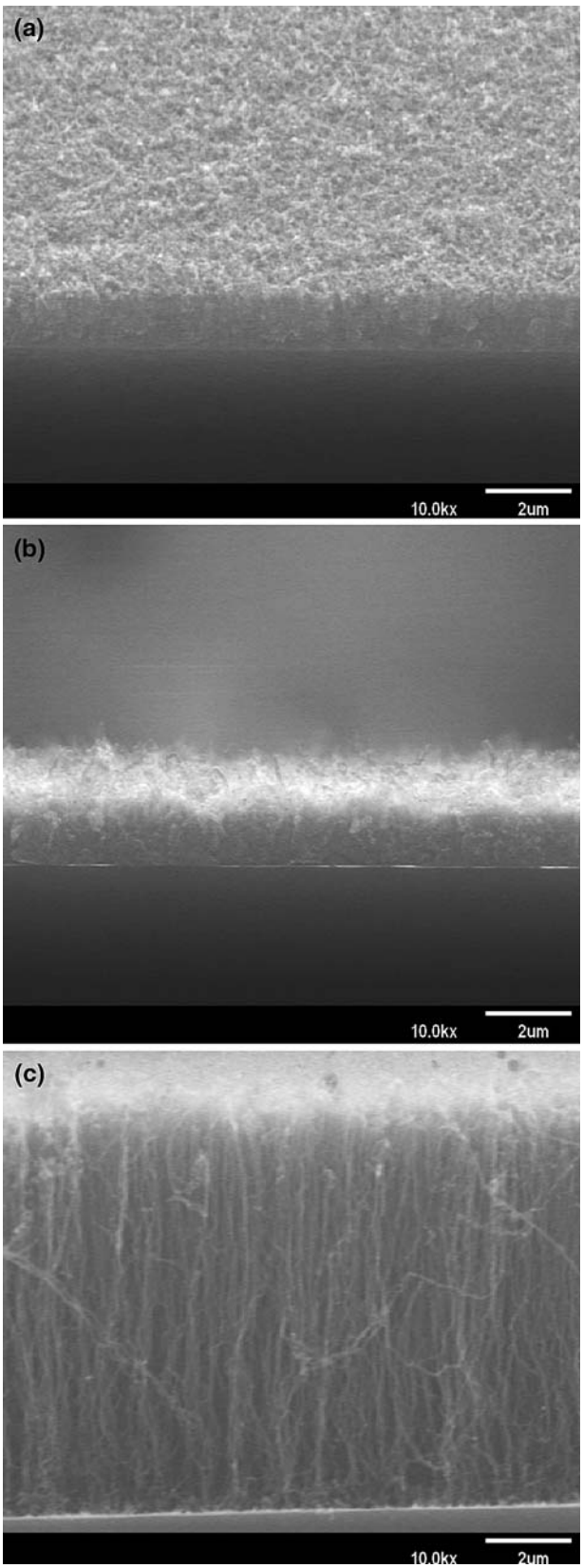

Fig. 3 SEM images of CNTs with various H_2 flow rate during plasma pretreatment of (**a**) 100, (**b**), 200 and (**c**) 300 sccm

only aggregates gradually but also etches via exciting H_2. Furthermore, the significantly long lifetime in the presence of H_2 can be explained by its gasification effect [23]. H_2 is beneficial to keep the exposed surface clean of carbon and prevent catalyst deactivation [24]. The size and distribution of these nanoparticles are dependent on the flow rate of H_2 during plasma pretreatment. This leads Ni particles to become smaller at the support of H_2 from the same temperature. Herein, it appears that a higher flow rate of H_2 plasma pretreatment favors the formation of uniform Ni nanoparticles from the SEM observations. Furthermore, the enhancement of H_2 gas [20] in plasma treatment can provide extra exciting H_2 (H^*). Therefore, much higher carbon productivity is obtained in the presence of H_2.

The structure of MWCNTs, which is obtained from the Ni catalyst particles treated by H_2 plasma at the flow rate of 300 sccm, is displayed in Fig. 4. An embryonic Ni catalyst particle is formed in the course of H_2 plasma pretreatment because of the difference of the interfacial energies between Ni catalyst particle/substrate and Ni catalyst particle/gas, with its catalytic decomposition of CH_4 to liberate carbon atoms. The change of elastic energy and surface energy of the carbon layer caused the radius of curvature of the Ni catalyst particle to become small. The rising gradient of the surface energy, then enhanced the surface diffusion of carbon atoms from the bottom to the top of the Ni catalyst particles. Therefore, significantly, a spindle-shaped Ni catalyst particle exists within the MWCNTs. The details of MWCNT growth mechanisms

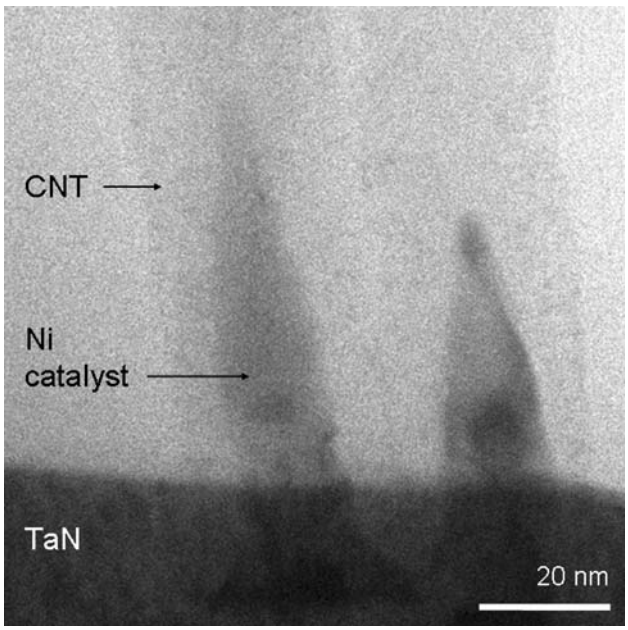

Fig. 4 TEM image of CNT synthesized with the H_2 flow rate during plasma pretreatment of 300 sccm

can be found elsewhere [25]. In addition, the TEM image reveals that there are well-graphitized layers, and the direction of graphite basal planes is parallel to the tube axis, as illustrated in Fig. 4.

Raman spectroscopy was used to investigate the vibrational characteristics of the carbon samples. Raman spectra of MWCNTs obtained at H_2 flow rate during plasma pretreatment of 100, 200, and 300 sccm are illustrated in Fig. 5. All the Raman spectra display two broad bands at 1,330 cm^{-1} (D-band) and 1580 cm^{-1} (G-band). The D-band is associated with the vibrations of carbon atoms with dangling bonds in plane terminations of "disordered graphite" or glassy carbons. The G-band corresponds to the E_{2g} mode of graphite and is related to the vibration of sp^2-bonded carbon atoms in the two-dimensional hexagonal lattice of the graphite layer. In addition, the G-band indicates the degree of crystallinity in the graphite structure, whereas the intensity of the D-band represents the impurities, defects, or lattice distortions in MWCNTs.

Ferrari and Robertson [26] proposed that the intensity ratio of G and D bands (I_D/I_G) is related to the sp^2 carbon cluster sizes in the graphene sheet and is nearly proportional to the defect density. The I_D/I_G ratio is 0.96, 0.92 and 0.84, respectively, which is shown in Fig. 6. This means that the MWCNTs present a lower degree of structural disorder by using H_2 plasma pretreatment. In fact, H_2 flow rate can promote the formation of uniform Ni nanoparticles, and then, to control the surface morphology of the catalyst film. Many parameters can influence the morphology of the catalyst (pretreatment time, power of rf or microwave, H_2 pressure, substrate temperature, catalyst film thickness and so on), in this study we kept all of them

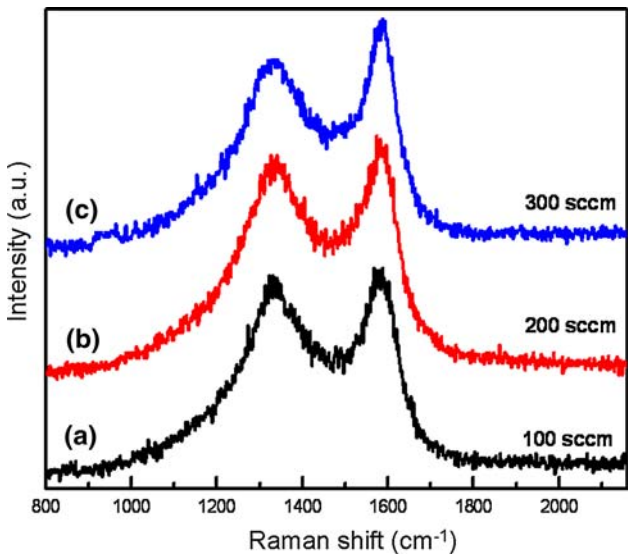

Fig. 5 Raman spectra of CNTs with various H_2 flow rate during plasma pretreatment. The Raman spectra of all samples show the D-band and G-band around 1,360 and 1,580 cm^{-1}, respectively

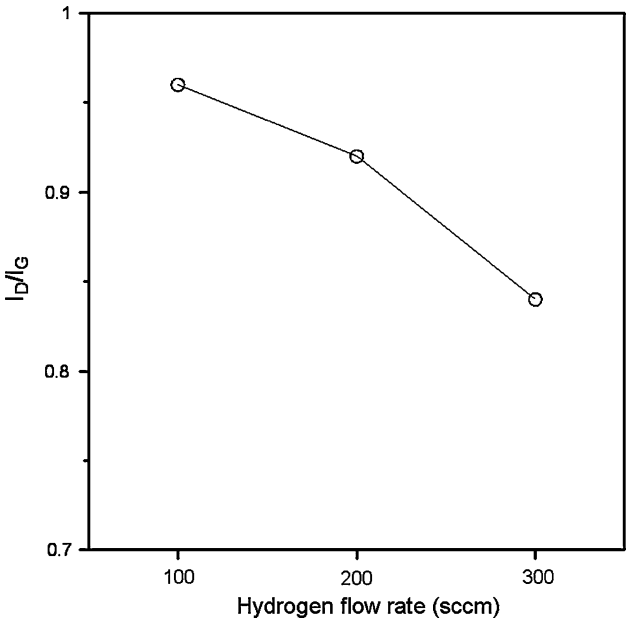

Fig. 6 I_D/I_G ratios of CNTs as a function of H_2 flow rate during plasma pretreatment

constant and only changed the flow rate in order to indirect check this case of Ni nanoparticles via H_2 plasma pretreatment. Results indicated that the I_D/I_G ratio decreases with increasing flow rate. From the analysis of Raman spectra, we observed that the higher flow rate induces the amorphization of the lattice and formation of defects in MWCNTs, indicating the decrease of the degree of disorder in MWCNTs. This result is consistent with the SEM observations. Actually, hydrogen is believed to influence the surface orientations of the catalyst by lattice re-structuring, which consequently influences the carbon deposit structure [27–30].

Conclusions

In summary, we combined SEM, Raman and TEM techniques to investigate the effects of H_2 flow rate during plasma pretreatment on the synthesis of the MWCNTs.

We synthesized MWCNTs by using MPCVD on Ni/TaN/Si substrates. From SEM observations, higher flow rates lead to denser Ni catalyst nanoparticles. In addition, the results of Raman spectra and TEM indicate that the morphologies of MWCNTs transform from amorphous carbon to a crystalline graphite structure or finite-sized graphite structure, depending on the H_2 flow rate during plasma pretreatment. A decrease in the number of defects and optimized morphologies therefore is believed to play a significant role in improving the field-emission characteristics observed in the future.

Acknowledgments This work was partially supported by the National Center for Theoretical Sciences of Taiwan and the National Science Council of Taiwan and I-Shou University, under Grants No. NSC97-2218-E-214-003, NSC96-2218-E-214-002, ISU97-07-01-04 and ISU97-02-20. Technical support from the National Nano Device Laboratories contract NDL-95S-C-067 is also acknowledged.

References

1. S. Iijima, Nature **354**, 56 (1991). doi:10.1038/354056a0
2. R.H. Baughman, A.A. Zakhidov, W.A. de Heer, Science **297**, 787 (2002). doi:10.1126/science.1060928
3. H.W.C. Postma, T. Teepen, Z. Yao, M. Grifoni, C. Dekker, Science **293**, 76 (2001). doi:10.1126/science.1061797
4. J. Kong, N.R. Franklin, C. Zhon, M.G. Chapline, S. Peng, K. Cho et al., Science **287**, 622 (2000). doi:10.1126/science.287.5453.622
5. B.H. Chen, H.C. Lin, T.Y. Huang, J.H. Wei, H.H. Wang, M.J. Tsai et al., Appl. Phys. Lett. **88**, 093502 (2006). doi:10.1063/1.2179612
6. Y.T. Jang, S.I. Moona, J.H. Ahnb, Y.H. Lee, B.K. Ju, Sensor Actuat. B **99**, 118 (2004). doi:10.1016/j.snb.2003.11.004
7. A.S. Teh, S.B. Lee, K.B.K. Teo, M. Chhowalla, W.I. Milne, D.G. Hasko et al., Microelectron. Eng. **67–68**, 789 (2003). doi:10.1016/S0167-9317(03)00140-0
8. C.P. Juan, C.C. Tsai, K.H. Chen, L.C. Chen, H.C. Cheng, Jpn. J. Appl. Phys. **44**, 2612 (2005). doi:10.1143/JJAP.44.2612
9. Y.H. Lee, Y.T. Jang, B.K. Ju, Appl. Phys. Lett. **86**, 173103 (2005). doi:10.1063/1.1915530
10. D.S. Bethune, C.H. Kiang, M.S. de Urief, G. Gorman, R. Savoy, J. Vazquez et al., Nature **363**, 605 (1993). doi:10.1038/363605a0
11. W.K. Maser, E. Muñoz, A.M. Benito, M.T. Martinez, G.F. de la Fuente, Y. Maniette et al., Chem. Phys. Lett. **292**, 587 (1998). doi:10.1016/S0009-2614(98)00776-3
12. Z.F. Ren, Z.P. Huang, J.W. Xu, J.H. Wang, P. Bush, M.P. Siegel et al., Science **282**, 1105 (1998). doi:10.1126/science.282.5391.1105
13. S. Gan, M.G. Chapline, N.R. Franklin, T.W. Tombler, A.M. Cassen, H. Dai, Science **283**, 512 (1999). doi:10.1126/science.283.5401.512
14. D.B. Geohegan, A.A. Puretzky, I.N. Ivanov, S. Jesse, G. Eres, Appl. Phys. Lett. **83**, 1851 (2003). doi:10.1063/1.1605793
15. Y.C. Choi, Y.M. Shin, Y.H. Lee, B.S. Lee, G.S. Park, W.B. Choi et al., Appl. Phys. Lett. **76**, 2367 (2000). doi:10.1063/1.126348
16. X. Ma, E.G. Wang, Appl. Phys. Lett. **78**, 978 (2001). doi:10.1063/1.1348319
17. T. de los Arcos, F. Vonau, M.G. Garnier, V. Thommen, H.G. Boyen, P. Oelhafen et al., Appl. Phys. Lett. **80**, 2383 (2002). doi:10.1063/1.1465529
18. H.C. Wen, K. Yang, K.L. Ou, W.F. Wu, R.C. Luo, C.P. Chou, Microelectron. Eng. **82**, 221 (2005). doi:10.1016/j.mee.2005.07.028
19. H. Neumayer, R. Haubner, Diam. Relat. Mater. **13**, 1191 (2004). doi:10.1016/j.diamond.2003.11.015
20. W.S. Choi, S.H. Choi, B. Hong, D.G. Lim, K.J. Yang, J.H. Lee, Mater. Sci. Eng. C **26**, 1211 (2006). doi:10.1016/j.msec.2005.09.037
21. C. Lautent, E. Flahaut, A. Peigney, A. Rousset, N. J. Chem. **22**, 1229 (1998). doi:10.1039/a801991f
22. Y.H. Wang, J. Lin, C.H.A. Huan, G.S. Chen, Appl. Phys. Lett. **79**, 680 (2001). doi:10.1063/1.1390314
23. Y. Zhixin, C. De, B. Tøtdal, A. Holmen, J. Phys. Chem. B **109**, 6096 (2005). doi:10.1021/jp0449760
24. J.H. Yen, I.C. Leu, C.C. Lin, M.H. Hon, Diam. Relat. Mater. **13**, 1237 (2004). doi:10.1016/j.diamond.2003.11.045
25. Z.Y. Juang, I.P. Chien, J.F. Lai, T.S. Lai, C.H. Tsai, Diam. Relat. Mater. **13**, 1203 (2004). doi:10.1016/j.diamond.2004.01.002
26. A.C. Ferrari, J. Robertson, Phys. Rev. B **61**, 14095 (2000). doi:10.1103/PhysRevB.61.14095
27. P.E. Anderson, N.M. Rodriguez, J. Mater. Res. **14**, 2912 (1999). doi:10.1557/JMR.1999.0389
28. P.E. Nolan, D.C. Lynch, A.H. Cutler, J. Phys. Chem. B **102**, 4165 (1998). doi:10.1021/jp980996o
29. P.E. Nolan, D.C. Lynch, A.H. Cutler, Carbon **32**, 477 (1994). doi:10.1016/0008-6223(94)90169-4
30. P.E. Nolan, M.J. Schabel, D.C. Lynch, A.H. Cutler, Carbon **33**, 79 (1995). doi:10.1016/0008-6223(94)00122-G